# EVALUATION OF THE INDIRECT TENSILE STRENGTH (ITS) OF CEMENT-TREATED CLAYEY SOILS USING XGBOOST PREDICTION MODEL

**Van-Ngoc Pham[1], Huu-Dao Do[1], Thi Phuong Khue Nguyen[1], Van-Khanh Tran[1,2], Dinh-Viet Le[1]***

[1]*The University of Danang - University of Science and Technology, Vietnam*

[2]*Tra Vinh University, Vietnam*

*Corresponding author: ldviet@dut.udn.vn

(Received: March 12, 2026; Revised: May 15, 2026; Accepted: June 05, 2026)

DOI: 10.31130/ud-jst.2026.24(7B).582E

**Abstract -** This study develops a data-driven framework using Extreme Gradient Boosting (XGBoost) to predict the Indirect Tensile Strength (ITS) of cement-treated clayey soils. Using 180 specimens with five input variables - cement content, curing time, curing temperature, plasticity index, and compaction energy - the model was trained (80%) and tested (20%), achieving strong accuracy (training $R^2$=0.932, RMSE=55.41 kPa; testing $R^2$=0.922, RMSE=81.98 kPa). SHapley Additive exPlanations (SHAP) analysis was applied for interpretability, showing cement content (39.3%) and curing time (30.1%) as the dominant predictors, followed by plasticity index (12.9%), while compaction energy (9.1%) and curing temperature (8.6%) had minor influence. K-means clustering combined with SHAP waterfall plots identified five distinct strength-development behavior groups, offering mechanistic insight into ITS variability. Overall, the XGBoost-SHAP framework proves to be a robust, interpretable tool for performance-based design and mixture optimization of cement-treated soils in infrastructure applications.

**Key words -** Cement-stabilized soil; indirect tensile strength; XGBoost; machine learning; SHAP; pavement engineering

## 1. Introduction

Cement-stabilized soils (CSS) have long been employed in transportation and geotechnical engineering as structural components in pavement subbases and bases, embankments, working platforms, and ground improvement systems. The addition of cement initiates hydration and secondary pozzolanic reactions, leading to the formation of cementitious bonds between soil particles. These physicochemical processes substantially improve stiffness, strength, and durability, thereby enhancing resistance to repeated traffic loading and adverse environmental conditions [1]. As a result, CSS has become an economical and technically viable solution, particularly in regions where in situ soils exhibit insufficient engineering performance.

Despite the recognized benefits in compressive strength and stiffness, the tensile behavior of cement-treated soils remains a critical factor governing long-term performance. In pavement systems, tensile stresses are commonly induced by moving wheel loads, thermal gradients, and shrinkage effects associated with cement hydration. These stresses often exceed the relatively low tensile capacity of stabilized soils, leading to crack initiation and propagation, which ultimately compromise structural integrity and service life [2, 3]. Consequently, reliable characterization of tensile resistance is essential for performance-based design and durability assessment of stabilized layers.

Direct tensile testing of soil–cement mixtures is inherently difficult due to specimen preparation challenges, stress alignment issues, and the absence of widely accepted standard procedures. In this context, the Indirect Tensile Strength (ITS) test has emerged as a practical and reproducible alternative. In this method, a cylindrical specimen is subjected to diametral compression, generating a nearly uniform tensile stress perpendicular to the loading direction. The ITS test provides a representative measure of tensile strength associated with cracking resistance and fatigue performance of stabilized geomaterials, and it has been widely adopted in both research and engineering practice [4].

Previous experimental investigations have demonstrated that ITS is influenced by a range of interacting parameters, including cement content, curing duration, curing temperature, soil plasticity, moisture condition, and compaction effort. These factors interact in a highly nonlinear manner, reflecting the complex coupling between physicochemical reactions and soil fabric evolution [5]. For instance, increasing cement content generally enhances bonding strength, while extended curing promotes continued hydration; however, their combined effects depend strongly on soil mineralogy and environmental conditions. Such complexity presents a significant challenge for developing generalized predictive relationships.

Traditional statistical approaches, particularly linear and multilinear regression models, have been widely used to estimate ITS based on experimental variables. While these methods offer simplicity and interpretability, they are often inadequate for capturing nonlinear interactions and higher-order dependencies among influencing factors [6]. This limitation has motivated the increasing adoption of machine learning (ML) techniques in civil engineering, where data-driven models can effectively learn complex input–output relationships without requiring predefined functional forms [7-10].

Among advanced ML algorithms, Extreme Gradient Boosting (XGBoost) has demonstrated superior performance in regression tasks involving nonlinear and heterogeneous datasets. Its ability to handle feature interactions, prevent overfitting through regularization, and provide robust predictive accuracy makes it particularly suitable for modeling the behavior of cement-treated soils.

Accordingly, this study develops a data-driven framework for predicting the ITS of cement-treated clayey soils using the XGBoost algorithm. An experimental database comprising key variables - cement content, curing time, curing temperature, plasticity index, and compaction energy - is utilized. The specific objectives are to: (i) establish a high-accuracy predictive model for ITS, (ii) perform a comprehensive parametric analysis to quantify the influence of individual factors and their interactions, and (iii) provide insights that support mixture design and optimization of stabilized soils for infrastructure applications. The findings are expected to contribute to the advancement of performance-based design methodologies in pavement and geotechnical engineering.

## 2. XGBoost and data preparation

XGBoost is a powerful machine learning technique that utilizes gradient boosting decision trees to perform predictions [11]. In order to determine the estimated output ($\hat{y}_i$) for a given sample, the model aggregates the prediction scores ($f_k(x_i)$) from all individual trees within the ensemble. The predicted output can be expressed as:

$$\hat{y}_i = \sum_{k=1}^{K} f_k(x_i) \quad , f_k \in \phi \tag{1}$$

where $K$ is the total number of trees and $\phi$ is the set of regression tree parameters.

During learning process, the XGBoost minimizes the objective function ($\Phi$). This function is defined as

$$\Phi = \sum_{i=1}^{n} l(y_i, \hat{y}_i) + \sum_{k=1}^{K} \Omega(f_k) \tag{2}$$

In which

$$\Omega(f_k) = \gamma T + \frac{1}{2}\lambda \|w\|^2 \tag{3}$$

where, $T$ and $w$ are the number of leaves and the norm of leaf weights, respectively. In addition, $\lambda$ and $\gamma$ are the Regularization parameters. This regularization framework prevents over-fitting and gives XGBoost a distinct advantage over traditional gradient boosting methods.

XGBoost constructs trees in a sequential and cumulative manner, where each new tree is trained to correct the errors of the preceding trees. To optimize the objective function efficiently, the algorithm employs a second-order Taylor expansion. This approach approximates the loss function using the first-order ($g_i$) and second-order ($h_i$) gradient statistics, allowing the model to find an optimal solution for the leaf node weights ($w_j^*$) and the corresponding structure score. Following to the Tree Construction and Splitting step, the algorithm uses a greedy approach to discover the optimal tree structure. It interactively evaluates all possible split points across the leaf nodes and selects the one that results in the maximum Gain. The Gain function can be expressed as:

$$Gain = \frac{1}{2}\left[\frac{G_L^2}{H_L+\lambda} + \frac{G_R^2}{H_R+\lambda} - \frac{(G_L+G_R)^2}{H_L+H_R+\lambda}\right] - \gamma \tag{4}$$

where $\frac{G_L^2}{H_L+\lambda}$ and $\frac{G_R^2}{H_R+\lambda}$ are the structural scores of the left and right subtrees, respectively; and $\frac{(G_L+G_R)^2}{H_L+H_R+\lambda}$ is the score when no split is made [12]. If the Gain is negative, the proposed split is rejected and the node is not further partitioned, effectively acting as an automatic pruning mechanism. The Gain calculation determines the reduction in the objective function after a split, helping the model decide if adding a new sub-tree is beneficial compared to the complexity cost (γ).

In general, the SHAP(SHapley Additive exPlanations) is used to evaluate the performance of XGBoost model. SHAP was introduced by Lundberg and Lee [13] as a unified framework for interpreting ML model predictions. The method is rooted in cooperative game theory, specifically the Shapley value concept attributed to Shapley [14]. For a model (*f*) and input instance (*x*), the SHAP value $\varphi_i$ for feature i-th represents the contribution of that feature to the prediction relative to the expected model output:

$$f(x) = \varphi_0 + \sum_i \varphi_i \tag{5}$$

where $\varphi_0 = E[f(x)]$ is the expected model output as base value.

SHAP values satisfy three desirable properties. First, local accuracy ensures that the sum of all SHAP values across every feature exactly equals the model's predicted output for a given sample. In other words, SHAP fully and completely accounts for each individual prediction without any remainder. Second, missing guarantees that any feature which has no influence on the prediction is automatically assigned a SHAP value of zero, meaning the method never credits or blames variables that play no role in the model's output. Third, consistency ensures that if a feature becomes more influential in the model and contributing more strongly to the prediction. In addition, the corresponding SHAP value will never decrease, so that the importance scores always faithfully and coherently reflect the true contribution of each variable.

In this study, the experimental dataset used consists of 180 specimens of cement-stabilized soil. The dataset was obtained from the study conducted by Yin et al [17, 18]. All specimens were prepared and tested under controlled conditions following ASTM D6931 for indirect tensile strength measurement. Specimen geometry (100 mm diameter, 63.5 mm height), compaction procedures, curing conditions, and testing protocols were kept consistent throughout the experimental program as reported in that study.Each specimen is characterized by five input features: cement content (%), curing time (days), curing temperature (°C), plasticity index (PI, %), and compaction energy (kJ/m³). The target variable is the ITS measured in kPa following the ASTM D6931 standard protocol. Table 1 summarizes the statistical characteristics of the dataset. Cement content ranges from approximately 5% to 15%, curing time from 1 to 360 days, and ITS values spanning from approximately 35 kPa to 1100 kPa, reflecting a broad range of mix design conditions. The wide variability across all features underscores the need for a flexible, nonlinear predictive model capable of capturing complex interactions.

***Table 1.*** *Summary of dataset for XGBoost model*

| Feature | Min | Max | Mean | Std. Dev. | Unit |
|---|---|---|---|---|---|
| Cement content | 2 | 15 | 6.27 | 3.48 | % |
| Curing time | 1 | 360 | 39.28 | 67.13 | days |
| Curing temperature | 20 | 60 | 25.93 | 10.71 | °C |
| Plasticity index | 10 | 46 | 17.09 | 5.58 | % |
| Compaction energy | 280 | 2680 | 931.60 | 742.08 | kJ/m³ |
| ITS (target) | 35.98 | 1104.66 | 338.58 | 209.53 | kPa |

The dataset was spitted into training (80%) and testing (20%) subsets using stratified random sampling to preserve the distributional characteristics of the target variable.

The 80:20 split ratio was selected following established practice in geotechnical ML research, as it provides adequate training coverage across the input feature space while preserving a statistically representative test set [13, 15, 16]. The XGBoost regression was implemented using the xgboost R-language library [15].

To ensure robust model performance and mitigate overfitting, a rigorous hyperparameter tuning process was implemented. The basis for selecting the optimal configuration was the minimization of the Root Mean Square Error (RMSE) on the validation sets, achieved through simultaneous Bayesian optimization integrated with a 5-fold cross-validation framework. This probabilistic approach iteratively evaluated predefined discrete search spaces to identify the most effective parameter combination. Specifically, the learning rate (η) was searched across $\{10^{-5}, 10^{-4}, 10^{-3}, 0.01, 0.02, 0.05, 0.1\}$. The maximum tree depth (*d*) was explored within {1, 3, 5, 10, 15, 20}. The regularization parameter was tested at {0, 0.001, 0.01, 0.1}. Furthermore, to control stochasticity during training, the subsample ratio and the column sampling rate per tree were evaluated across {0.8, 0.98} and {0.8, 0.86, 1.0}, respectively. Finally, the total ensemble sizes (*T*) was assessed among {50, 100, 300, 500}. By systematically navigating these specific tuning ranges, the Bayesian optimizer effectively identified the configuration that maximized the model's predictive accuracy and generalizability

In addition, the performance of XGBoost model was evaluated using three metrics: the coefficient of determination ($R^2$), RMSE, and MAE. $R^2$ measures the proportion of variance in ITS explained by the model, while RMSE and MAE quantify prediction error in absolute units (kPa).

Figure 1 presents the hyperparameter performance matrix, illustrating the evaluation of the $R^2$ metric of test set across varying learning rates (η), maximum tree depths (d), and ensemble sizes (T). A comprehensive analysis of the heatmaps reveals several distinct behavioral trends of the model. First, models constrained to a minimal depth (*d* = 1) consistently exhibit severe underfitting, yielding the lowest $R^2$ scores across all configurations.

Conversely, increasing the tree depth beyond 10 leads to performance saturation, where $R^2$ values plateau and marginally decline, indicating an onset of overfitting without contributing to better generalization. Second, the interaction between the learning rate and the number of trees demonstrates that extremely low learning rates (e.g., $10^{-5}$ and $10^{-4}$) fail to achieve convergence within the given iterations, particularly when ensemble sizes (*T*) is small. The optimal balance between learning capacity and generalization is distinctly localized. The hyperparameter search space culminates in a clear performance peak at ensemble sizes (*T*) of 100, maximum tree depth (*d*) of 3, column sampling rate per tree of 0.8, subsample ratio of 0.8 and learning rate (η) = 0.05, which achieves the highest Test $R^2$ of 0.9222. This specific configuration is therefore concluded to be the most optimal, as it effectively captures the underlying data patterns while avoiding both underfitting and excessive model complexity.

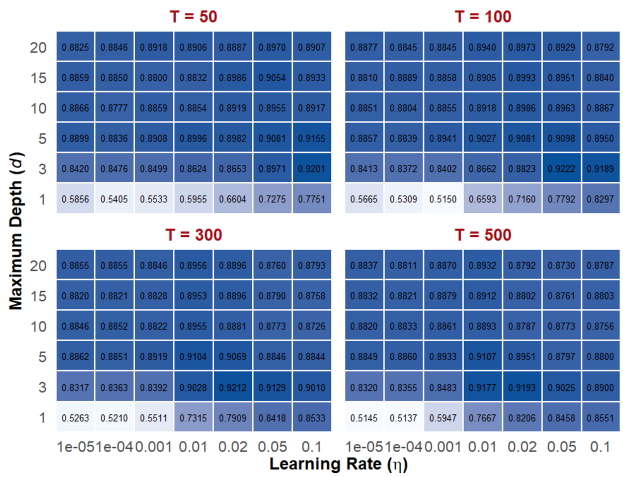


***Figure 1.*** *Hyperparameter tuning matrix showing Test $R^2$ of XGBoost across learning rate (η), maximum tree depth (d), and number of estimators (T)*

## 3. Results and Discussion

### *3.1. XGBoost Performance*

Figure 2 presents the scatter plot of the predicted versus actual ITS values for the XGBoost model during the training phase. The model demonstrates a strong learning capability, achieving an $R^2$ of 0.932, an RMSE of 55.41 kPa, and an MAE of 42.1 kPa. The tight clustering of data points around the ideal 1:1 reference line indicates a high degree of accuracy in capturing the underlying relationships within the training dataset. This confirms that the algorithm effectively learns the complex, nonlinear interactions between the input variables - such as cement content, curing time, and soil plasticity characteristics - and the resulting indirect tensile strength.

Figure 3 illustrates the model's performance on the unseen testing set, serving as a critical evaluation of its generalization ability. The XGBoost model maintains robust predictive accuracy, yielding an $R^2$ of 0.9222, alongside an RMSE of 81.98 kPa and an MAE of 55.9 kPa. While these error metrics are slightly higher than those of the training set - a typical outcome in machine learning - the closely matched $R^2$ scores indicate that the model does not suffer from significant overfitting. However, as observed in the testing plot, the model exhibits a noticeable tendency toward under-prediction at extreme ITS values (particularly >800 kPa). This phenomenon is consistent with the general behavior of gradient boosting models, which often struggle to extrapolate beyond the dense regions of the training data distribution. Nevertheless, the overall results demonstrate that the XGBoost approach is highly reliable for predicting ITS development in cement-stabilized soils.

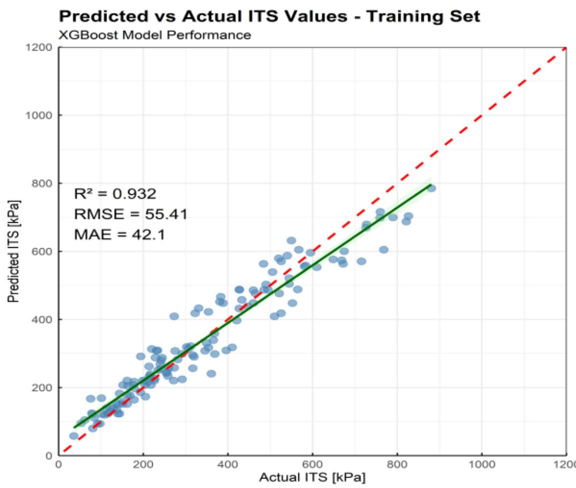


***Figure 2.*** *Comparison of actual and predicted ITS values using the XGBoost model for the training set*

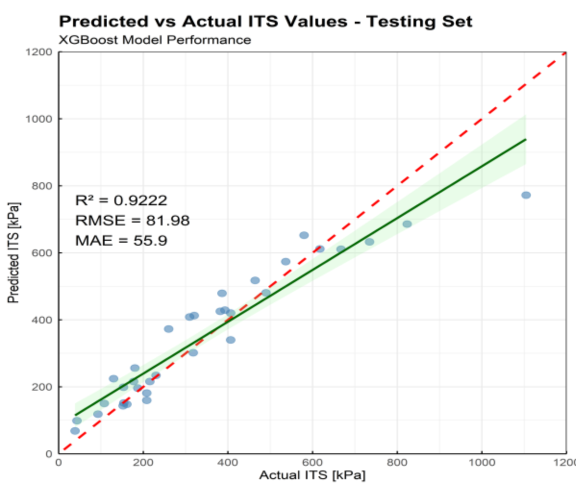


***Figure 3.*** *Comparison of actual and predicted ITS values using the XGBoost model for the testing set*

Figure 4 presents the SHAP summary plot, providing a comprehensive analysis of both the magnitude and direction of each feature's contribution to the model's predictions. Cement content emerges as the dominant predictor, with a mean absolute SHAP value of 103.249 kPa. The plot demonstrated the strong positive correlation where high cement content substantially enhance the predicted ITS, reflecting the central role of the cement-soil matrix and pozzolanic reactions in strength development. In addition, the curing time is the second most influential factor (mean |SHAP| = 79.082 kPa), displaying a distinctive non-linear pattern: strength increases rapidly during early stages but eventually reaches a plateau, which is consistent with the known kinetics of cement hydration.

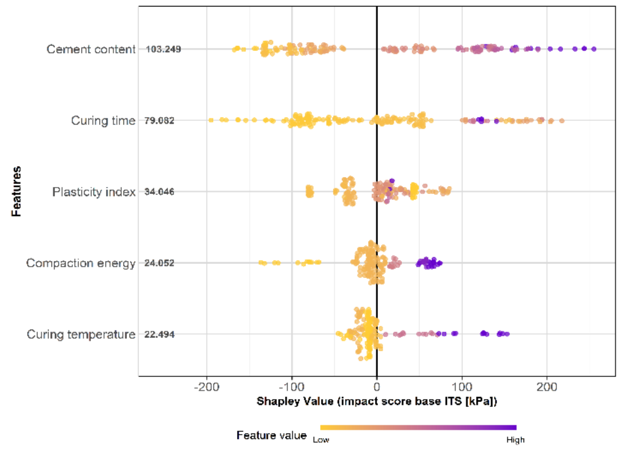


***Figure 4.*** *The distribution of SHAP values for each feature in the XGBoost model*

### *3.2. Variable Contribution Analysis*

The relative importance of input variables, quantified SHAP contribution percentages (Figure 5), indicates that cement content and curing time are the two dominant factors governing ITS, contributing 39.3% and 30.1%, respectively. The remaining variables - including plasticity index (12.9%), compaction energy (9.1%) and curing temperature (8.6%) - exhibit comparatively smaller but still non-negligible effects.

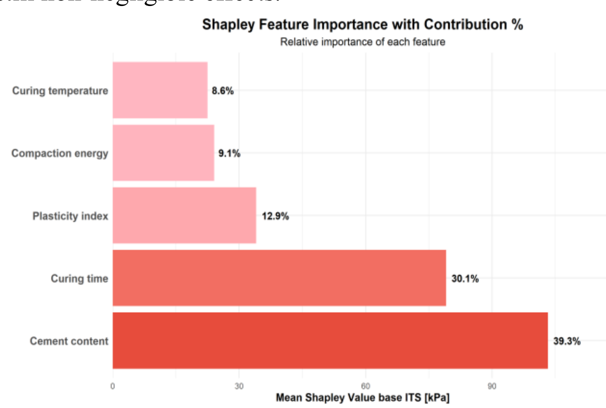


***Figure 5.*** *The feature importance plot with percentage contributions of each feature in the prediction model of ITS*

Cement content emerged as the most influential parameter, accounting for 39.3% of the mean Shapley value contribution to ITS, reflecting a strong nonlinear enhancement effect particularly at low to moderate dosages. This behavior is attributable to the progressive formation and densification of the soil–cement matrix through pozzolanic and cementitious reactions. Nevertheless, the marginal gain in ITS tends to diminish at higher cement contents, implying the existence of an optimal dosage range beyond which additional cement yields limited benefit.

Curing time ranked second in importance with a contribution of 30.1%, exhibiting a pronounced positive effect on ITS development. The rapid strength gain observed during early curing stages is associated with active hydration and cementation processes, while the rate of increase gradually decelerates as the microstructure approaches a stable configuration.

Plasticity index contributed 12.9% to the overall feature importance, representing a secondary yet meaningful influence on the efficiency of cement stabilization. Soils with lower plasticity indices generally achieved higher ITS values owing to more effective interfacial bonding, whereas high-plasticity soils tend to constrain the availability of cementitious products and thereby limit strength development.

Compaction energy and curing temperature contributed 9.1% and 8.6%, respectively, representing the least influential parameters among those considered. Compaction energy plays a role in improving density and interparticle contact, with its effect being more pronounced at lower cement contents where cementation is not yet the dominant strength mechanism. Curing temperature, while beneficial in accelerating early-stage hydration, exerts a moderate and nonlinear influence, with diminishing returns under elevated thermal conditions. The comparable magnitudes of these two parameters suggest that their roles are largely supplementary relative to the dominant contributions of cement content and curing time.

Overall, the SHAP-based analysis highlights that ITS is primarily governed by chemical stabilization mechanisms (cement content and curing time), while physical and environmental factors provide secondary, modifying effects.

## 4. Cluster Group Analysis

The XGBoost model uses K-means clustering to divide the data into five distinct groups. Figures 6–10 present SHAP waterfall plots for each group, illustrating how different features contribute to the predictions. Zoomed-in images highlight the unique patterns specific to each cluster.

Figure 6 shows that Group 1 is mainly characterized by strong negative SHAP contributions from both cement content and curing time. The cement content in this cluster lies below the dataset average, leading to negative SHAP contributions. In contrast, compaction energy and curing temperature have only minor effects on the predicted ITS. This pattern represents a set of samples with low cement content and short curing time, which leads to ITS values below the average. This result is fully consistent with the observed trend.

In Figure 7, Group 2 clearly shows positive SHAP contributions, mainly driven by compaction energy. In contrast, cement content and curing time exhibit bidirectional effects, as they can both increase and decrease the predicted ITS. Notably, in some samples, these two factors act in opposite directions: when cement content contributes positively, curing time tends to reduce the predicted value, and vice versa.

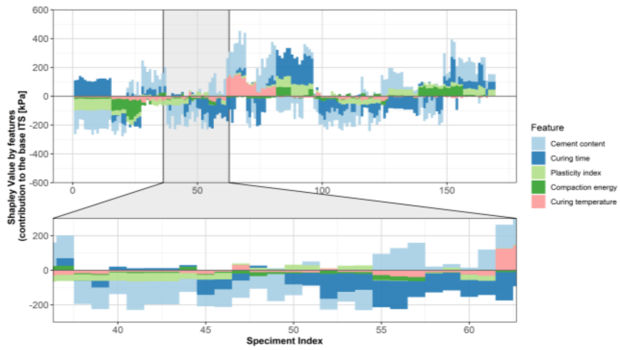


***Figure 6.*** *The SHAP waterfall plot for Cluster Group 1*

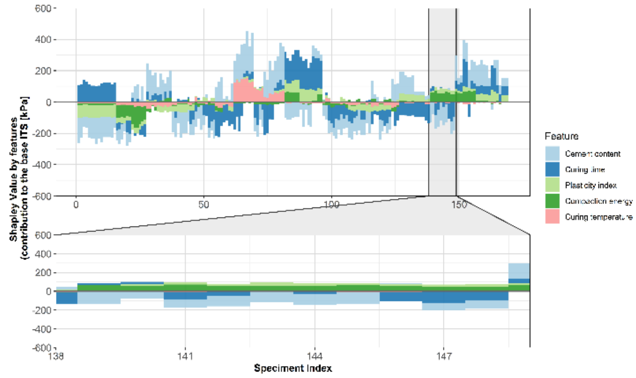


***Figure 7.*** *The SHAP waterfall plot for Cluster Group 2*

According to Figure 8, Group 3 is characterized by negative SHAP contributions from both curing time and cement content, indicating that these two factors tend to reduce the predicted ITS. Meanwhile, the remaining variables, including curing temperature, plasticity index, and compaction energy, show negligible effects, with SHAP values fluctuating around zero. Therefore, they do not play a significant role in the variation of ITS.

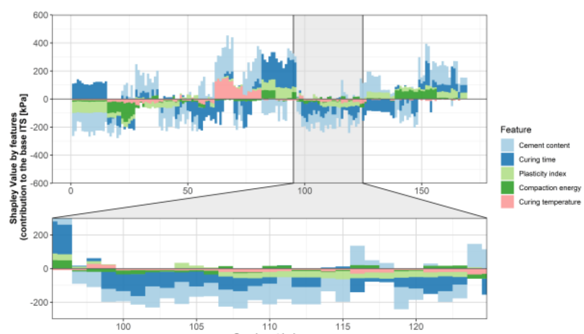


***Figure 8.*** *The SHAP waterfall plot for Cluster Group 3*

As shown in Figure 9, Group 4 is characterized by negative SHAP contributions from all five input variables. This pattern represents a set of samples with low cement content and short curing time, where the two main strength-controlling factors have not yet reached their effective levels. In addition, the negative contributions from curing temperature, plasticity index (PI), and compaction energy further reinforce this decreasing trend, resulting in systematically low predicted ITS values.

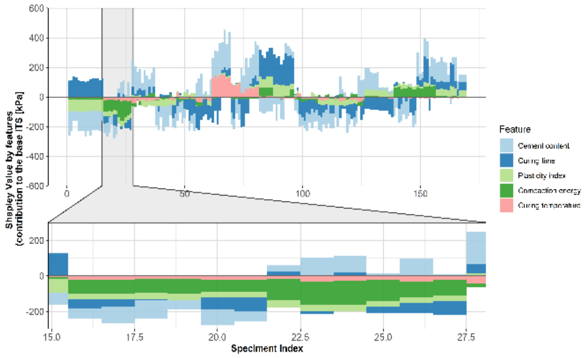


***Figure 9.** The SHAP waterfall plot for Cluster Group 4*

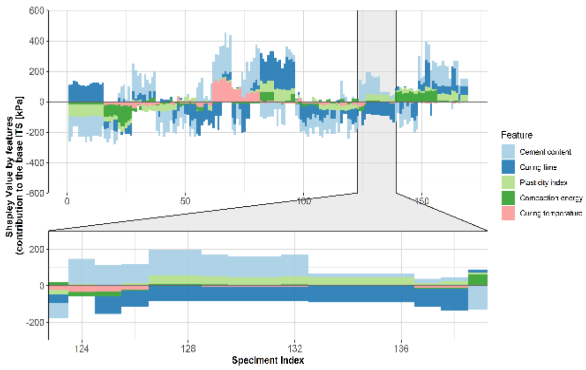


***Figure 10.** The SHAP waterfall plot for Cluster Group 5*

In Figure 8, Group 5 is characterized by positive SHAP contributions mainly from curing time, while cement content shows a strong negative effect. This contrast reflects a group of samples with low cement content but long curing duration, where the cumulative effect of hydration partially compensates for the lack of cement.

## 5. Conclusion

This study developed an XGBoost model to predict the Indirect Tensile Strength (ITS) of cement-treated clay using 180 specimens and five input variables. The model achieved strong performance (training: $R^2$=0.932, RMSE=55.41 kPa, MAE=42.1 kPa; testing: $R^2$=0.922, RMSE=81.98 kPa, MAE=55.9 kPa). SHAP analysis identified cement content (39.3%) as the most influential factor, showing diminishing returns at higher dosages, followed by curing time (30.1%), reflecting hydration kinetics. Plasticity index (12.9%) affected stabilization efficiency, with lower-plasticity soils achieving better bonding. Compaction energy (9.1%) mattered mainly at low cement contents, while curing temperature (8.6%) had the weakest, largely supplementary influence. K-means clustering combined with SHAP waterfall plots revealed five distinct behavioral groups, showing low-strength cases driven by insufficient cement/curing time, compensatory effects of compaction energy, and extended curing offsetting low cement content. Limitations include reliance on a single 180-point dataset, lack of benchmarking against other algorithms, SHAP's inability to establish causality, and untested applicability to field conditions. Future work will expand datasets, compare multiple models, and pursue field validation.

## REFERENCES

[1] J. K. Mitchell, K. Soga, and C. O'Sullivan, *Fundamentals of soil behavior*. John Wiley & Sons, 2025.

[2] J. Mallela, H. V. Quintus, and K. Smith, Consideration of lime-stabilized layers in mechanistic-empirical pavement design, *The National Lime Association,* vol. 200, no. 1, pp. 1-40, 2004.

[3] K. Lemaire, D. Deneele, S. Bonnet, and M. Legret, Effects of lime and cement treatment on the physicochemical, microstructural and mechanical characteristics of a plastic silt, *Engineering Geology*, vol. 166, pp. 255-261, 2013.

[4] W. R. Hudson and T. W. Kennedy, "*An indirect tensile test for stabilized materials,*" Center for Highway Research, The University of Texas at Austin, Austin, TX, USA, Research Report No. 98-1, 1968.

[5] F. Sariosseiri and B. Muhunthan, Effect of cement treatment on geotechnical properties of some Washington State soils, *Engineering geology*, vol. 104, no. 1-2, pp. 119-125, 2009.

[6] D. Xuan, L. Houben, A. Molenaar, and Z. Shui, Mechanical properties of cement-treated aggregate material–a review, *Materials & Design*, vol. 33, pp. 496-502, 2012.

[7] M. A. Shahin, M. B. Jaksa, and H. R. Maier, Artificial neural network applications in geotechnical engineering, *Australian geomechanics,* vol. 36, no. 1, pp. 49-62, 2001.

[8] H. Moayedi, M. Mosallanezhad, A. S. A. Rashid, W. A. W. Jusoh, and M. A. Muazu, A systematic review and meta-analysis of artificial neural network application in geotechnical engineering: theory and applications, *Neural Computing and Applications*, vol. 32, no. 2, pp. 495-518, 2020.

[9] Q.-C. Truong and A.-T. N. Vu. "Machine Learning Applications for Chloride Ingress Prediction in Concrete: Insights from Recent Literature". *The University of Danang - Journal of Science and Technology*, vol. 22, no. 11B, pp. 91-97, 2024, doi:10.31130/ud-jst.2024.528E.

[10] T. T. H. Truong and V. D. A. Huynh, Estimating resilient modulus of subgrade soils using bagging-based ensemble model, *The University of Danang - Journal of Science and Technology*, vol 5, no. 114.2, pp. 6-10, 2017.

[11] T. Chen and C. Guestrin, "XGBoost: A scalable tree boosting system," in *Proceedings of the 22nd ACM SIGKDD International Conference on Knowledge Discovery and Data Mining*, San Francisco, CA, USA, Aug. 13–17, 2016. New York, NY, USA: ACM, 2016, pp. 785–794. https://doi.org/10.1145/2939672.2939785.

[12] T. Nguyen, D.-K. Ly, T. Q. Huynh, and T. T. Nguyen, Soft computing for determining base resistance of super-long piles in soft soil: A coupled SPBO-XGBoost approach, *Computers and Geotechnics,* vol. 162, p. 105707, 2023, doi: 10.1016/j.compgeo.2023.105707.

[13] S. M. Lundberg and S.-I. Lee, A unified approach to interpreting model predictions, *in Advances in Neural Information Processing Systems,* vol. 30, 2017, pp. 4765–4774.

[14] L. S. Shapley, A value for n-person games, *in Contributions to the Theory of Games,* vol. 2, no. 28, pp. 307–317, 1953.

[15] Y. Liu and A. Just, SHAPforxgboost: SHAP plots for XGBoost, R package version 0.1.0, *github.com,* 2020. [Online]. Available: https://github.com/liuyanguu/SHAPforxgboost/ [Accessed March 01, 2026]

[16] B.-Q.-V. Nguyen, T.-H. Nguyen, and V.-C. Le, "An advanced machine learning-based mathematical equation for predicting compression index from readily available soil physical properties," *Geomechanics and Geoengineering*, vol. 20, no. 4, pp. 788–804, 2025. https://doi.org/10.1080/17486025.2025.2455109.

[17] K. Yin, N. H. Dong, L. Li, W. Zhang, and J. Xu, Indirect tensile strength of cement-treated soil under diverse curing conditions: From experimental characterization to prior-fitted transformer-based prediction, *Transportation Geotechnics*, vol. 61, Art. no. 102098, 2026.

[18] N. H. Dong and K. Yin, "Indirect tensile strength of cement-stabilized soils: a hybrid experimental and literature dataset," *Mendeley Data*, version 3, Mar. 20, 2026. [Online]. Available: https://doi.org/10.17632/gf5n7nb7hj.3 [Accessed March 01, 2026].